Macrocyclic diphosphine ligands in asymmetric carbon–carbon bond-forming reactions

Michael Widhalm [a,*], Petra Wimmer [a], Gerd Klintschar [b]

[a] Institut für Organische Chemie, Universität Wien, Währingerstraße 38, A-1090 Wien, Austria
[b] Institut für Physikalische Chemie, Universität Graz, Heinrichstraße 28, A-8010 Graz, Austria

Abstract

Seven chiral macrocyclic ligands with potential O_2P_2 and N_2P_2 coordination sites owing their chirality from the incorporation of an axial–chiral binaphthyl unit were used as chiral auxiliaries in transition metal catalyzed carbon–carbon bond-forming reactions. Three model reactions were investigated, and enantioselectivities are discussed on the basis of accepted mechanistic pathways by using X-ray structural analyses.

1. Introduction

During the past decade progressively extensive studies have focused on the formation of asymmetric quaternary carbon centers under the catalysis of chiral transition metal complexes. A large number of reports has been published, and these are summarized in review articles and books [1,2]. Highlights have been palladium and nickel catalyzed cross-coupling reactions with ferrocene ligands affording 3-phenyl-1-butene and biaryls with up to 94 and 95% e.e. respectively [3,4]. Also palladium catalyzed allylic substitution reactions have been realized very successfully using P–P, P–N and N–N ligands [5].

These results encouraged us to investigate the dependence of the asymmetric induction on the distance between the asymmetric moiety and the transition metal center. Simple model compounds like 2A–6A [6a,b] or 10A and 11A were therefore tested in typical catalytic reactions. A local C_S symmetry of the diphosphine sub-unit with cis P-phenyl groups constitutes an achiral array near the transition metal. A chiral "disturbance" is introduced by a C_2-symmetrical binaphthyl unit which is held at varying distance from the transition metal center by means of two polymethylene ("spacer")

chains, thus introducing different degrees of chiral interaction. It is obvious that a direct relationship between asymmetric induction and the distance between the chiral center and transition metal is based on a rough simplification, because the existence of a preferred conformation of the spacer determines the actual distance. Therefore the expected correlation will only be observed if high conformative flexibility of the polymethylene chain and unrestricted access of reactants to the complexation sites exist.
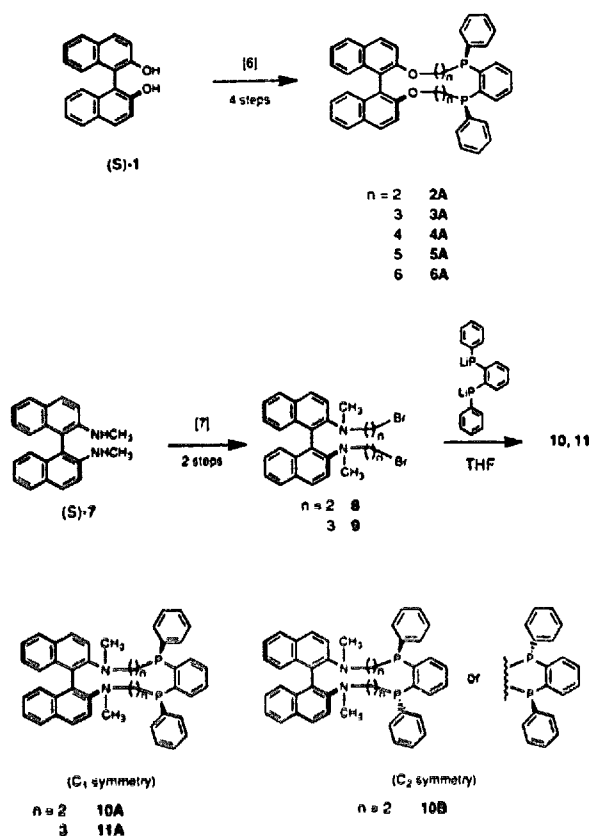
In addition to dioxa–diphospha ligands, diaza–diphospha ligands were also investigated since the introduction of nitrogen donor atoms might improve the efficiency of the catalysts; one of the nitrogen atoms may offer an additional complexation site during the catalytic cycle, thus lowering the risk of side reactions of coordinatively unsaturated species and forcing the metal into the center of the macrocycle. Moreover, the $N–CH_3$ groups could interact with the incoming substrate resulting in a preorganisation before any association step or oxidative addition were to take place.

2. Results and discussion

2.1. Synthesis of ligands and complexes

Macrocycles 10 and 11 with phosphorus and nitrogen donor atoms were prepared from dibromides 8 and 9 [7]

---

* Corresponding author.

(S)-1

n = 2	2A
3	3A
4	4A
5	5A
6	6A

(S)-7

| n = 2 | 8 |
| 3 | 9 |

(C₁ symmetry)

| n = 2 | 10A |
| 3 | 11A |

(C₂ symmetry)

| n = 2 | 10B |

Scheme 1.

respectively, and yielded either a single diastereoisomer with C_1 symmetry (11A) or a mixture of diastereoisomers which were separated on deactivated silica gel [7] (10A and 10B). All ligands proved to be sufficiently stable to enable their purification and handling under air without precautions. Enantiopure samples of the macrocycles were prepared from the optically active precursor (=)(S)-7 in the same way.

From C_1-symmetrical ligands, nickel(II) complexes were isolated. Treatment of 10A or 11A with $NiCl_2$ afforded orange-brown crystalline products. Both complexes showed similar NMR spectra and, moreover, from 11A · $NiCl_2$ an X-ray structure analysis could be obtained which revealed a slightly distorted square-planar complex geometry without coordination of nitrogen atoms (see below). Accordingly, we assume the exclusive or at least predominant operation of a P–P coordinated complex of 11A during catalysis. In the case of 10A · $NiCl_2$, however, the (presumable) P–P coordinated nickel complex was isolated in low yield; formation of N–P coordinated complexes cannot be excluded since the nitrogen atoms are in an appropriate geometric arrangement.

2.2. X-ray structural analysis

From one ligand (2A) and two of the complexes (2A · $PdCl_2$ and 11 · $NiCl_2$) the crystal structures could

be determined. Characteristic structural features are listed in Table 1.

The biaryl angles range from 112.13° for 2A to 76.22° for 11A · $NiCl_2$. As observed previously, these pronounced changes occur easily in 1,1'-binaphthyl series and are caused by the flat energy minimum between the cisoid and transoid conformation at approximately 65 and 115° respectively [6b,c,d]. The ease of conformational changes during coordination to nickel(II) or palladium(II) and an "out of center" torsion of the P_2MCl_2 (M = Ni, Pd) fragment, which resulted in a nearly perpendicular arrangement of the macrocycle and the complex unit, seem to compensate for the presumptive steric strain, thus stabilizing these complexes. The only evidence for steric strain was found in deviations of carbons 14–11–61–64 from linearity by 1.0/5.4° (2A) to 6.91/3.16° (2A · $PdCl_2$). Both complexes show a slightly distorted square-planar array with typical angles and distances and no nitrogen coordination in 11A · $NiCl_2$.

2.3. Asymmetric catalysis

The present paper deals with three catalytic carbon–carbon coupling reactions with different mechanistic

Table 1
Selected data from crystal structure analyses [a]
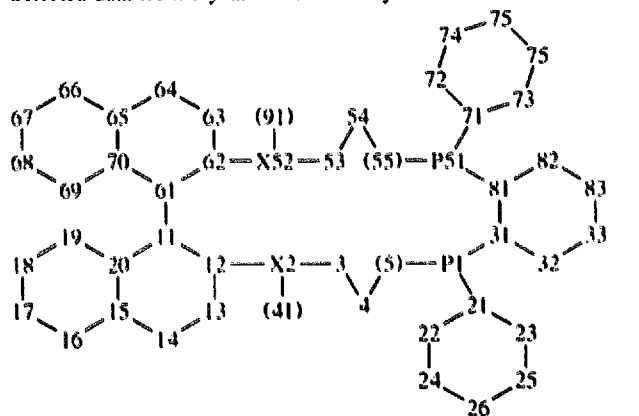
X = O, N
General labeling scheme for crystal structures

	2A	2A · PdCl₂	11A · NiCl₂
Biarylangle	112.13°	101.57°	76.22°
"Out of cycle torsion" of the metal complex [b]	–	99.3°	83.03°
P1–M–P51	–	86.88°	88.62°
P1–M	–	2.210	2.134
P51–M	–	2.205	2.134
P1–P51	3.219	3.036	2.982
C1A–M–C1B		95.54°	94.72°
C1A–M	–	2.351	2.185
C1B–M	–	2.347	2.199
14–11–61	1.0°	–6.9°	6.5°
64–61–11	5.4°	–3.2°	–3.2°
P1–31–81–P51	4.9°	0.8°	5.7°

[a] Distances in Å. [b] The angle between best planes through the macrocyclic perimeter (11–12–X2–3–4–(5–)P1–P51–(55–)54–53–X52–62–61) and the complex subunit (P1–M–P51).
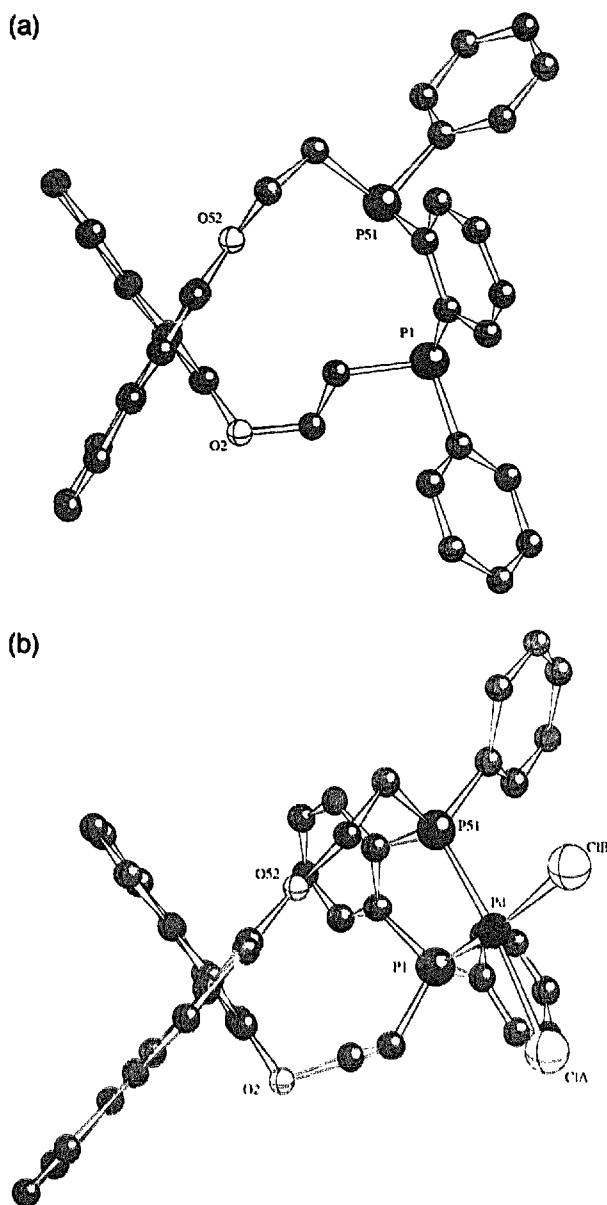
(a)

(b)

Fig. 1. (a) Crystal structure of ligand **2A**; hydrogen atoms and solvent molecules have been omitted for clarity. (b) Crystal structure of the palladium complex **2A·PdCl₂**; hydrogen atoms and solvent molecules have been omitted for clarity.

features which, according to proposed mechanisms, require chiral interaction in different sectors of the surrounding space [8–10].

Reaction (1), the cross-coupling reaction between 1-phenylethyl magnesium chloride and vinyl bromide under catalysis of nickel complexes, affords 3-phenyl-1-butene (**12**). Reaction (2) yields a homologue, 4-phenyl-1-pentene (**13**), which is obtained by reaction of 1-phenylethyl magnesium chloride with allyl phenyl ether. Reactions (3) are allylic substitutions with dimethyl malonate as nucleophile.

Table 2 lists isolated yields and enantiomeric excesses (e.e., in parentheses) of reactions (1)–(3) using

Model Reactions for Asymmetric Carbon-Carbon Coupling
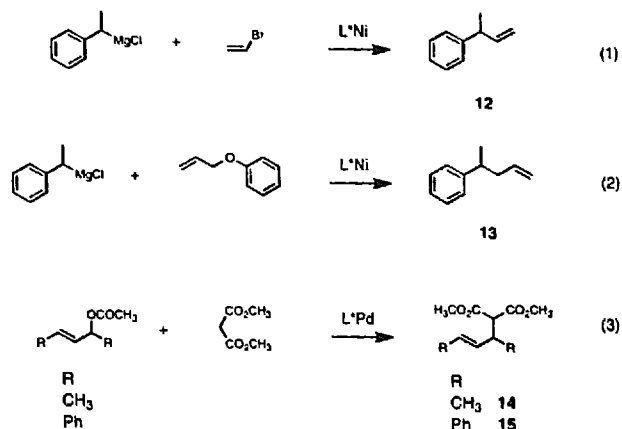
Scheme 2.

ligands with $(S)_{axial}$-configuration. Reaction (1) was conducted following a standard procedure [8a] with slight modifications. The product was isolated in moderate to good yield but asymmetric inductions were found to be low. Also, for reaction (2) the enantioselectivities were low and no dependence of the asymmetric induction from the length of the spacer was observed. The best result was obtained at 0 °C with ligand **4A**, yielding 75% of (S)-**13** with 23% e.e. The allylic substitution reaction (3) (R = phenyl) afforded the product in good chemical yields and showed the expected dependence of e.e. from the length of the spacer group for **2A–6A**. Under all conditions investigated so far the (R)-enantiomer predominates if ligands with $(S)_{axial}$-configuration are employed. A decrease of e.e. from 84

Table 2
Asymmetric carbon–carbon coupling reactions [a]

Entry	Ligand [b]	Reaction (1) [c]	Reaction (2) [d]	Reaction (3) [e]
1	2A	50 (1S)	71 (8R)	83 (84R)
2	3A	67 (9S)	73 (14R)	71 (50R)
3	4A	84 (6S)	79 (15S) [f]	77 (31R)
4	5A	89 (4R)	73 (12R)	87 (11R)
5	6A	76 (7R)	73 (5S)	77 (17R)
6	10A	62 (0) [g]	79 (1S)	75 (52R)
7	11A	54 (16R)	75 (6S)	41 (77R) [h]

[a] Isolated yield (enantiomeric excess, absolute configuration). [b] The absolute configuration was $(S)_{axial}(S,R)_0$ as depicted in Scheme 1; symmetry C_1. [c] Scheme 2, reaction (1): vinyl bromide (7.1 mmol), 1-phenylethyl magnesium chloride (11.8 mmol), NiCl₂ (0.5 mol%), ligand (0.5 mol%), solvent Et₂O, 20 h, 0°C (Section 3.5.1). [d] Scheme 2, reaction (2): allyl phenyl ether (20 mmol), 1-phenylethyl magnesium chloride (20 mmol), NiCl₂ (0.2 mol%), ligand (0.2 mol%), solvent Et₂O, 4–20 h (TLC), RT (Section 3.5.2). [e] Scheme 2, reaction (3): (E)-1,3-diphenylprop-3-ene-1-yl acetate (1 mmol), dimethyl malonate (3 mmol), BSA (3 mmol), KOAc (catalytic amount), [Pd(η³-C₃H₅)Cl]₂ (1 mol%), ligand (1 mol%), solvent CH₂Cl₂, 4–18 h, RT (Section 3.5.3). [f] At 0°C 75 (23S). [g] At 10°C. [h] No complete conversion obtained.
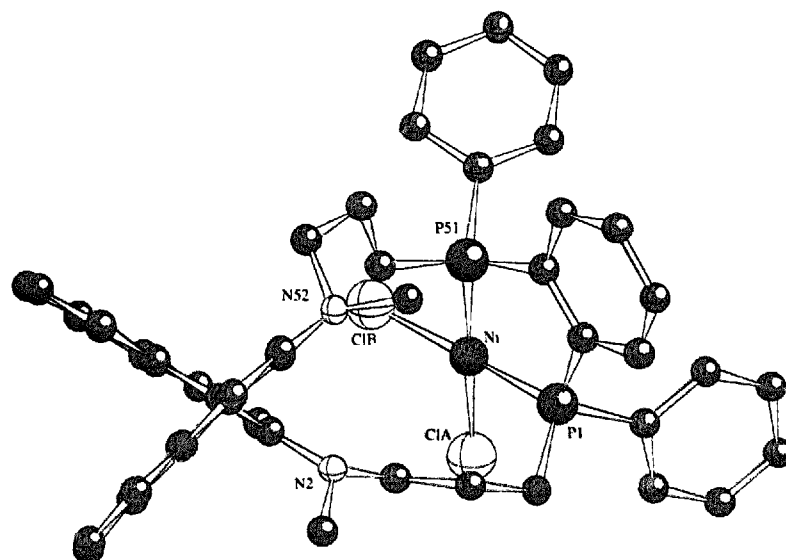
Fig. 2. Crystal structure of the nickel complex 11A · NiCl₂: hydrogen atoms and solvent molecules have been omitted for clarity.

Table 3
Allylic substitution [a] (reaction (3))

Entry	Substrate	Ligand [b]	Base	Reaction time [c]	Yield [d]	E.e. [e] (configuration)	Notes [f]
1	R = Ph	2A	BSA	1 h	83	84 (R)	
2	R = Ph	3A	BSA	5 h	71	50 (R)	
3	R = Ph	4A	BSA	18 h	77	31 (R)	
4	R = Ph	5A	BSA	18 h	87	11 (R)	
5	R = Ph	6A	BSA	20 h	77	17 (R)	
6	R = Ph	10A	BSA	4 h	78	52 (R)	
7	R = Ph	11A	BSA	20 h	41	77 (R)	
8	R = Ph	2A	NaH	18 h	89	82 (R)	
9	R = Ph	3A	NaH	6 h	82	37 (R)	
10	R = Ph	4A	NaH	6 h	85	16 (R)	
11	R = Ph	5A	NaH	6 h	85	10 (R)	
12	R = Ph	6A	NaH	6 h	81	5 (R)	
13	R = Ph	10A	NaH	4 h	99	59 (R)	
14	R = Ph	11A	NaH	4 h	83	77 (R)	
15	R = Ph	2A	BSA	18 h	91	84 (R)	volume 4 ml
16	R = Ph	2A	BSA	1 h	83	86 (R)	Pd₂(dba)₄
17	R = Ph	2A	BSA	2 days	~ 10	...	Pd(OAc)₂
18	R = Ph	3A	BSA	2 days	74	52 (R)	0°C
19	R = Ph	2A	BSA	18 h	81	79 (R)	[Lig.] = 0.5 mol%
20	R = Ph	2A	BSA	18 h	85	85 (R)	[Lig.] = 2 mol%
21	RCH₃	2A	BSA	24 h	85	21 (+)	
22	RCH₃	2A	BSA	24 h	83	23 (+)	0°C
23	RCH₃	2A	BSA	24 h	64	24 (+)	– 10°C
24	RCH₃	2A	BSA	18 h	84	20 (+)	solvent DMF
25	RCH₃	2A	BSA	18 h	83	15 (+)	solvent CH₃CN
26	RCH₃	10A	BSA	18 h	84	< 1	
27	RCH₃	11A	BSA	18 h	54	33 (+)	

[a] Scheme 2, reaction (3), entries 1–7, 15–25, see Table 1, footnote [e]; entries 8–14 (E)-1,3-diphenylprop-2-ene-1-yl acetate (1 mmol), dimethyl malonate (1.5 mmol), sodium hydride (1.5 mmol), L* · PdCl₂ (1 mol%), solvent THF, RT (Section 3.5.4). [b] The absolute configuration was (S)ₐₓᵢₐₗ(S,R)ₚ as depicted in Scheme 1. [c] Entries 1–20 were monitored by TLC and stopped either if no starting material could be detected or if no progress could be noticed. [d] Isolated yield. [e] Estimated by using shift experiments (Eu(hfc)₃) and HPLC (Chiralcel OD-H) (entries 1–20) or by chiral GC (Octakis(6-O-methyl-2,3-di-O-pentyl)-γ-cyclodextrin) and shift experiments (Eu(hfc)₃) (entries 21–27). [f] Variation of standard procedures.

to 17% is observed within the group of homologues. In contrast to these ligands, **10A** and **11A** with N-CH₃ instead of O showed the opposite behavior; **11A** (77% e.e.) exhibits a significantly higher efficiency than **10A** (52% e.e.). We speculated that this reversal could be due to the presence of more than one catalytically active palladium complex of **10A**.

Since reaction (3) seemed to be sufficiently sensitive to structural variations, additional experiments were made to extend the scope and limitations of the new auxiliaries (Table 3). If N,O-bis(trimethylsilyl)acetamide (BSA) was substituted by NaH, enantiomeric excesses are somewhat lower but a similar trend is observed. In these experiments isolated $PdCl_2$ complexes of **2A-6A** [6a,b] were used, which were found to give better reproducible results. We also noticed an effect previously reported by Allen et al. [11], that the concentration of reactants influenced the rate of the reaction significantly while the e.e. remained unaffected; with BSA in 1 ml of CH_2Cl_2 the conversion was completed

within 1 h but the same reaction in 4 ml of CH_2Cl_2 took about 18 h to go to completion (entries 9, 15). In addition to $[Pd(C_3H_5)Cl]_2$, $Pd_2(dba)_4$ [12] (dba = $C_6H_5-CH=CH-CO-CH=CH-C_6H_5$) and $Pd(OAc)_2$ were also tested as sources for palladium. $Pd_2(dba)_4$ showed slightly higher e.e. with good chemical reactivity, but $Pd(OAc)_2$ proved to be largely unreactive (entries 1, 16, 17). Lowering the reaction temperature decreased the reaction rate dramatically, but the asymmetric induction was only slightly improved (entries 9, 18). Finally, the ligand/Pd ratio was varied (entries 19 (0.5 : 1), 8 (1 : 1), 20 (2 : 1)). The results pointed to a 1 : 1 complex as the catalytically active species with an equilibrium constant above 1. These results encouraged us to extend our investigations to allylic substrates without phenyl groups, like (E)-pent-3-ene-2-yl acetate (**14**) and 3-acetoxy-cyclohex-1-ene, both substrates for which reports of high asymmetric induction are rare [13]. Using our most efficient ligand, **2A**, **14** was obtained in good chemical yield (85%), but the e.e. was

a)

$\pi-\sigma-\pi$

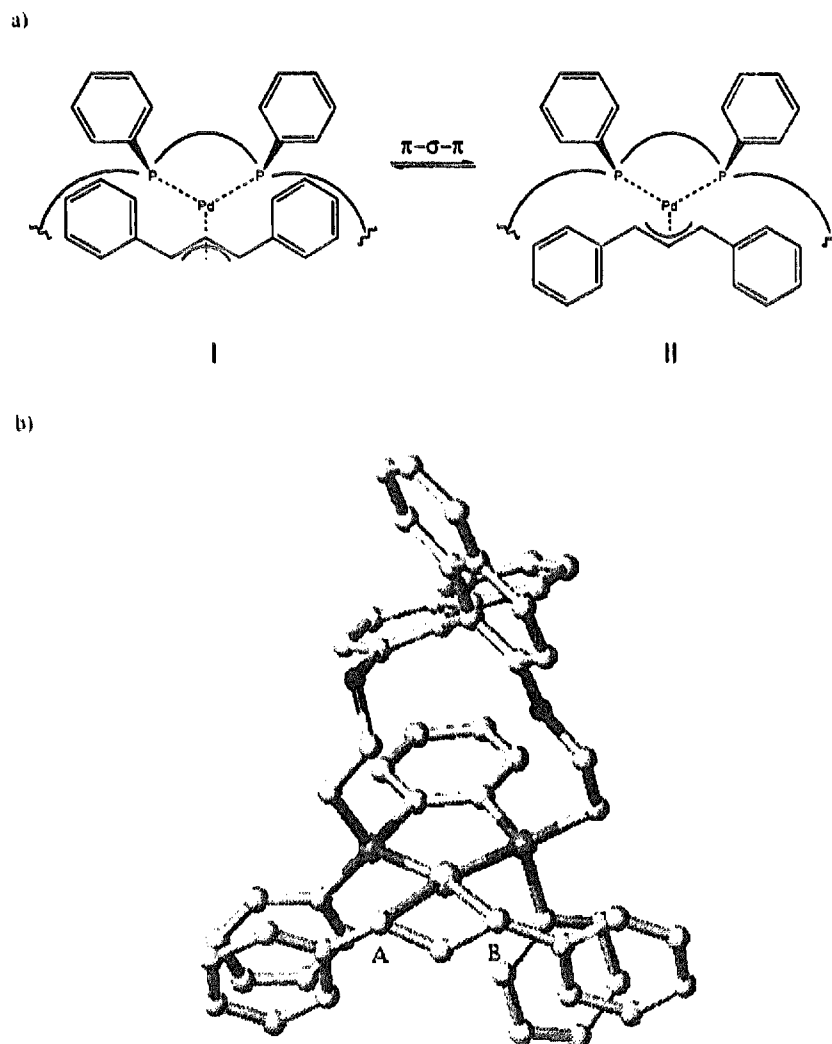I   II

b)

Fig. 3. (a) Diastereomeric intermediates interconvertible via a $\pi-\sigma-\pi$ mechanism. (b) Schematic representation of the presumptive predominating allylic intermediate in a Pd-2A catalyzed allylic alkylation.

low (21%). This result could not be improved significantly either by lowering the temperature (entries 21–23) or by varying the solvent (entries 21, 24, 25). A slightly higher asymmetric induction could be achieved with 11A (33% e.e.), while 10A failed to give any enantioselectivity (entries 26, 27). The reaction with the cyclic substrate 3-acetoxy-cyclohex-1-ene proceeded smoothly with good chemical yield, but with almost no enantioselectivity (not included in Table 2).

Despite the limited number of experiments the striking differences in the enantioselection exhibited in three C–C coupling reactions is worth consideration. We think that this behavior can be rationalized on the basis of different mechanistic suggestions for (1)–(3), as reported in the literature [8–10].

Model reactions (1) and (2), where chiral Grignard reagents are involved, generally differ from (3). In reactions (1) and (2) the configuration determining step is the enantioselective formation of an alkyl metal intermediate with both carbon fragments σ-bound to the metal center. This is followed by reductive elimination of the product with retention of the configuration. On the contrary, in reaction (3) the nucleophile attacks the terminal carbon atom of a π-allyl complex from "outside".

Since in (1) and (2) the enantiodetermining step is the selective reaction of one enantiomeric form of the Grignard reagent, this reaction is usually considered as a kinetic optical resolution [8a]. In both cases a diorganometal complex in which the asymmetric center is already fixed precedes the reductive elimination of the product. For reaction (1), proceeding under the catalysis of ferrocenyl-N=P ligands, a mechanism was proposed which postulates a weak N=Mg interaction to account for high enantioselectivity [8a]; in contrast, an epimerisation of the chiral carbon center via β-hydride elimination has also been discussed [8a,14]. If no appropriate donor atom in the ligand structure is available, only transient steric interactions of the Grignard reagent with the chiral carbon back-bone may operate to induce some enantiodifferentiation. Tentatively, we assume that this stereoselective association step is responsible for the e.e. rather than a difference in reactivity of the diastereomeric diorganometal intermediates. Suggestions for a mechanism of (2) are sparse, but π-allyl intermediates are most likely to be involved [9b]. Nevertheless, it seems to be a common feature of both cases that only a trajectory which is chirally modelled in an ideal manner will direct selectively one enantiomeric nucleophile to the reaction center.

For coupling (3), for which a different mechanism was suggested [10], the situation is much more promising. Since a non-chiral nucleophile attacks the symmetrical allyl intermediate from "outside", i.e. opposite the transition metal without preceding coordination at the metal center, the enantioselectivity of the overall reaction is governed by two features: (a) the preferred geometry of the allyl complex (Fig. 3(a) I and II) and (b) the regioselectivity of the nucleophilic attack.

From molecular modelling calculations we gained some evidence for a positive interaction between the 1,3-diphenyl-allyl moiety and the P-phenyl rings, which may be responsible for a highly preferred steric arrangement of the π-allyl complex [15]. This hypothesis is corroborated by the dramatic drop in e.e. if the corresponding dimethyl-allyl substrate is employed. Since the terminal carbon atoms of the allyl fragment are ca. 3 Å distant from each other, good regioselectivity caused by different steric interactions is relatively easily attained. A hypothetical structure of the preferred intermediate with $(S)_{axial}$-configuration is depicted in Fig. 3(b), showing a significantly better accessibility of the A-labeled allylic carbon from which an (R)-configurated product arises.

3. Experimental details

3.1. General procedures

M.p.: Kofler Heiztisch-Mikroskop (uncorrected). NMR: Bruker AC 250 F, AM 400 WB; unless otherwise noted spectra were recorded in CDCl$_3$ at 250.13 and 400.13 MHz respectively (^{1}H), 100.62 MHz (^{13}C{^{1}H}, J-modulated), and 161.98 MHz (^{31}P{^{1}H}). Abbreviations: br, broad; p, pseudo. Chemical shifts δ are given in parts per million relative to TMS (^{1}H, ^{13}C) and 85% H$_3$PO$_4$ (^{31}P). Phosphorus–carbon coupling constants (J_{cp}) were identified by comparison of ^{13}C NMR spectra recorded at 62.90 and 100.62 MHz respectively. MS: Varian MAT-CH7; FAB-MS: Finnigan MAT-95. Polarimeter: Perkin-Elmer 241 ($d = 1$ dm, thermostatted). Elemental analyses: Mikroanalytisches Laboratorium der Universität Wien.

3.2. Solvents and reagents

THF was distilled from potassium benzophenone ketyl, Et$_2$O from LiAlH$_4$ and CH$_2$Cl$_2$, acetonitrile and DMF were distilled from CaH$_2$. DMF was stored over molecular sieves (4 Å). Ethyl acetate (EE) was distilled, petroleum ether (b.p. 60–70 °C, PE) was used as purchased. All the other solvents were analytical grade. TLC: TLC-aluminium sheet silica gel 60, F$_{254}$ (Merck). Column chromatography: silica gel 60, 230–400 mesh ASTM (Merck); for the separation of diastereomers silica gel was dried for two days at 140–160 °C. A calculated amount of water was added with shaking and the adsorbant was allowed to stand for two days to reach homogeneity.

Allylphenylether [16], tetrakis(dibenzylideneaceton)-dipalladium(0) [12], 1,2-bis(phenylphosphino)benzene

[17], N,O-bis(trimethylsilyl)acetamide (BSA, distilled, Fluka), n-butyl lithium (solution 1.6 M in hexane, Merck), di-μ-chloro-bis-η³-allylpalladium(II) (Strem), (E)-pent-3-ene-2-yl acetate [18], (E)-1,3-diphenylprop-3-ene-1-yl acetate [19], dimethyl malonate (Aldrich, 99 + %), nickel chloride and nickel chloride hexahydrat (Aldrich, 99%), palladium(II)acetate (Strem, 97%), 1-phenylethyl chloride [20], sodium hydride (dispersion, 55–60%, Fluka), tris-[3-(heptafluoropropylhydroxy-methylene)-d-camphorato]-europium [Eu(hfc)₃] (Sigma), vinyl bromide (Aldrich, 98%).

3.3. Preparation of macrocyclic diaza–diphospha ligands (10 and 11)

3.3.1. General procedure

A Schlenk tube was carefully dried and charged with 20 ml of dry THF. After degassing by three freeze–pump–thaw cycles, 1,2-bis(phenylphosphino)benzene (353 mg, 333 μl, 1.2 mmol) was added and subsequently ^{n}BuLi solution (1.5 ml, 2.4 mmol) was added dropwise over 15 min. In a second Schlenk tube a degassed solution of 1 mmol of bromoamine [7] (526 mg of 8, 554 mg of 9) in 18 ml of THF was prepared. These two solutions were slowly and synchronously added to a well stirred volume of approximately 100 ml of degassed THF [7], avoiding excess of one of the reactants (1–1.5 h). After the addition was complete stirring was continued for 1 h and the solvent was evaporated. Water was added and the mixture was extracted with 3 × 20 ml of CH₂Cl₂. The combined extracts were washed with water and brine and dried (Na₂SO₄). After removal of the solvent under vacuo the residue was purified by column chromatography as given below.

3.3.2. 1,10-Dimethyl-4,7-diphenylbenzo[c]dinaphtho-[2,1-k:1′,2′-m]-1,10-diaza-4,7-diphosphacyclotetradeca-5,11,13-triene (10)

The crude mixture contained isomers 10A and 10B which were separated on deactivated silica gel (15% (w/w) H₂O, 65 g, PE/CH₂Cl₂ 65:35).

10A. 339 mg (52%).¹H NMR δ: 1.91 (m, 1H), 2.19 (s, 3H), 2.32 (s, 3H), 2.30–2.54 (m, 3H), 3.17 (m, 3H), 3.61 (m, 1H), 6.85 (m, 1H), 7.02–7.17 (m, 7H), 7.21–7.44 (m, 11H), 7.50 (m, 2H), 7.59 (d, 1H, *J* 8.9 Hz), 7.75 (d, 1H, *J* 8.9 Hz), 7.78 (d, 1H, *J* 8.9 Hz), 7.82 (d, 1H, *J* 7.9 Hz), 7.92 (d, 1H, *J* 8.9 Hz) ppm. ¹³C NMR δ: 26.64 (CH₂, dd, J_{CP} 5.3, 15.2 Hz), 29.07 (CH₂, dd, J_{CP} 2.6, 13.1 Hz), 41.72 (CH₃), 42.21 (CH₃), 52.27 (CH₂, d, J_{CP} 17.3 Hz), 54.41 (CH₂, dd, J_{CP} 5.5, 29.3 Hz), 120.25 (CH), 122.26 (CH), 123.51 (CH), 124.04 (CH), 125.68 (CH), 125.79 (CH), 126.14 (CH), 126.49 (CH), 127.39 (C), 127.59 (CH), 127.84 (CH), 128.09 (CH), 128.18 (CH), 128.32 (2CH), 128.43 (CH, d, J_{CP} 5.9 Hz), 128.50 (CH, d, J_{CP} 6.0 Hz), 128.60 (CH),

128.84 (CH), 129.58 (C), 129.71 (C), 130.76 (C), 132.27 (CH, d, J_{CP} 6.5 Hz), 132.39 (CH, d, J_{CP} 17.1 Hz), 132.81 (CH, d, J_{CP} 17.6 Hz), 132.86 (CH, d, J_{CP} 8.1 Hz), 134.35 (C), 134.52 (C), 138.38 (C, dd, J_{CP} 9.8, 15.0 Hz), 138.52 (C, dd, J_{CP} 7.7, 14.5 Hz), 143.57 (C, dd, J_{CP} 13.2, 30.1 Hz), 146.94 (C, dd, J_{CP} 12.2, 31.4 Hz), 148.53 (C), 150.15 (C) ppm. ³¹P NMR δ: −23.9, −21.8 (AB-system, J_{AB} 134.9 Hz) ppm. MS (170 °C): 658 (M⁺, 17%). Anal. Found: C, 79.20; H, 6.43; N, 4.15. C₄₄H₄₀N₂P₂ Calc.: C, 80.22; H, 6.12; N, 4.25%.

(S)-10A: $[\alpha]_\lambda^{20}$ −414 (589 nm), −435 (578 nm), −516 (546 nm), −1167 (436 nm) {c = 1.1, CH₂Cl₂}.

10B. 66 mg (10%). ¹H NMR δ: 2.21 (s, 6H), 2.33–2.51 (m, 4H), 3.04 (m, 2H), 3.39 (m, 2H), 7.04 (d, 2H, *J* 8.4 Hz), 7.11–7.30 (m, 16H), 7.41 (d, 2H, *J* 8.9 Hz), 7.46 (m, 2H), 7.79 (d, 2H, *J* 8.4 Hz), 7.84 (d, 2H, *J* 8.9 Hz) ppm. ¹³C NMR δ: 29.74 (CH₂, t, J_{CP} 13.6 Hz), 41.01 (CH₃), 53.52 (CH₂, d, J_{CP} 29.8 Hz), 121.61 (CH), 123.87 (CH), 125.85 (CH), 126.19 (CH), 127.24 (CH), 127.77 (CH), 128.04 (CH, d, J_{CP} 4.6 Hz), 128.58 (CH), 128.90 (C), 129.26 (CH, d, J_{CP} 9.2 Hz), 130.39 (C), 130.87 (CH, d, J_{CP} 16.3 Hz), 134.28 (C), 138.24 (CH, br d, J_{CP} 31.4 Hz), 139.71 (C, d, J_{CP} 13.2 Hz), 144.35 (C, br m), 150.65 (C) ppm. ³¹P NMR δ: −14.1 (br s) ppm. MS (180 °C): 658 (M⁺, 5%). Anal. Found: C, 78.96; H, 5.90; N, 4.12. C₄₄H₄₀N₂P₂ Calc.: C, 80.22; H, 6.12; N, 4.25%.

(S)-10B: $[\alpha]_\lambda^{20}$ −237 (589 nm), −248 (578 nm), −292 (546 nm), −598 (436 nm) {c = 1.2, CH₂Cl₂}.

3.3.3. 1,12-Dimethyl-5,8-diphenylbenzo[f]dinaphtho-[2,1-m:1′,2′-o]-1,12-diaza-5,8-diphosphacyclohexadeca-6,13,15-triene (11A)

The crude product was purified by chromatography on silica gel (PE/EE 95:5) to give 11A: 350 mg (51%); the racemic ligand was recrystallized from CH₂Cl₂/Et₂O; m.p. 289–291 °C. ¹H NMR δ: 0.52 (m, 1H), 0.97 (m, 1H), 1.57–1.78 (m, 2H), 1.83 (m, 1H), 1.90–2.12 (m, 2H), 1.97 (s, 3H), 2.19 (m, 1H), 2.55 (m, 2H), 2.65–2.72 (m, 1H), 2.68 (s, 3H), 2.88 (m, 1H), 6.54 (d, 1H, *J* 8.9 Hz), 6.76 (m, 1H), 6.98 (d, 1H, *J* 8.5 Hz), 7.07 (d, 1H, *J* 8.7 Hz), 7.14 (m, 4H), 7.21 (m, 1H), 7.25–7.35 (m, 12H), 7.41 (m, 1H), 7.59 (d, 1H, *J* 8.9 Hz), 7.76 (d, 1H, *J* 7.9 Hz), 7.81 (d, 1H, *J* 8.1 Hz), 7.91 (d, 1H, *J* 8.9 Hz) ppm. ¹³C NMR δ: 22.79 (CH₂, dd, J_{CP} 5.1, 8.8 Hz), 24.52 (CH₂, d, J_{CP} 19.9 Hz), 25.21 (CH₂, dd, J_{CP} 3.0, 15.5 Hz), 26.05 (CH₂, d, J_{CP} 17.3 Hz), 39.40 (CH₃), 41.62 (CH₃), 55.98 (CH₂, d, J_{CP} 8.7 Hz), 57.20 (CH₂, d, J_{CP} 13.3 Hz), 121.06 (CH), 121.32 (CH), 123.29 (CH), 123.87 (CH), 125.87 (2CH), 126.08 (CH), 126.41 (CH), 126.91 (C), 127.25 (CH), 127.63 (CH), 127.75 (CH), 128.12 (CH), 128.15 (CH, d, J_{CP} 5.1 Hz), 128.40 (2CH), 128.42 (CH, d, J_{CP} 5.0 Hz), 128.62 (CH), 129.00 (C), 129.05 (CH), 129.56 (C), 130.46 (C), 131.12 (CH, d, J_{CP} 15.5 Hz), 132.31 (CH, d, J_{CP} 8.1 Hz), 133.38 (CH, d, J_{CP} 19.1 Hz),

133.45 (CH), 134.68 (C), 134.87 (C), 137.14 (C, dd, J_{CP} 10.0, 15.7 Hz), 140.98 (C, dd, J_{CP} 5.2, 14.6 Hz), 144.12 (C, dd, J_{CP} 14.4, 30.1 Hz), 148.60 (C, dd, J_{CP} 14.0, 33.7 Hz), 148.85 (C), 151.01 (C) ppm. ^{31}P NMR δ: -25.1, -19.8 (AB-system, J_{AB} 151.2 Hz) ppm. MS (280 °C): 686 (M$^+$, 19%); FAB-MS: 687.5 (M$^+$H, 100%); the isotopic pattern observed is as expected for $C_{46}H_{45}N_2P_2$.

(S)-11A: $[\alpha]_x^{20}$ -309 (589 nm), -324 (578 nm), -380 (546 nm), -772 (436 nm) {$c = 1.1$, CH_2Cl_2}.

3.4. Preparation of nickel complexes

3.4.1. General procedure

To a solution of 0.07 mmol of the ligand in 1 ml of CH_2Cl_2 was added dropwise a solution of NiCl$_2 \cdot 6H_2O$ (17 mg, 0.07 mmol) in ethanol (2 ml). More ethanol (2–4 ml) was added carefully and the solution was allowed to stand undisturbed at RT. The nickel complexes crystallized during 24 h and were separated, washed with a little ethanol and dried in vacuo.

3.4.2. (1,10-Dimethyl-4,7-diphenylbenzo[e]dinaphtho-[2,1-k:1',2'-m]-1,10-diaza-4,7-diphosphacyclotetra-deca-5,11,13-triene)nickel(II)-dichloride (10A · NiCl$_2$)

20 mg (36%, small orange–brown crystals). ^{1}H NMR (CD$_2$Cl$_2$) δ: 2.40 (m, 2H), 2.44 (s, 3H), 2.69 (s, 3H), 3.08 (m, 1H), 3.17 (m, 1H), 3.29 (m, 1H), 3.67 (m, 2H), 3.85 (m, 1H), 6.69 (d, 1H, J 9.4 Hz), 6.95 (d, 1H, J 8.4 Hz), 7.00 (d, 1H, J 8.9 Hz), 7.10 (m, 2H), 7.28 (m, 4H), 7.39 (m, 4H), 7.50 (m, 4H), 7.60 (m, 4H), 7.67 (d, 1H, J 8.9 Hz), 7.72 (d, 1H, J 8.9 Hz), 7.75 (d, 1H, J 8.9 Hz), 7.86 (d, 1H, J 7.9 Hz), 8.01 (d, 1H, J 8.9 Hz) ppm. ^{13}C NMR (CD$_2$Cl$_2$) δ: 24.71 (CH$_3$, t, J_{CP} 15.9 Hz), 25.05 (CH$_3$, t, J_{CP} 16.4 Hz), 40.10 (CH$_2$), 41.21 (CH$_2$), 49.32 (CH$_2$, t, J 3.0 Hz), 51.12 (CH$_2$), 121.31 (CH), 123.17 (CH), 124.22 (CH), 124.31 (CH), 125.78 (CH), 126.06 (CH), 126.19 (CH), 126.42 (CH), 126.51 (C), 127.57 (C), 127.88 (CH), 128.12 (CH), 128.52 (CH), 129.15 (CH, t, J_{CP} 5.4 Hz), 129.20 (CH, t, J_{CP} 5.4 Hz), 129.45 (CH), 130.18 (C), 130.45 (C), 131.09 (CH, t, J_{CP} 8.8 Hz), 131.56 (CH), 131.60 (CH), 131.78 (C, t, J_{CP} 50.3 Hz), 131.85 (C, t, J_{CP} 50.6 Hz), 132.10 (CH, t, J_{CP} 18.0 Hz), 132.27 (CH, t, J_{CP} 4.3 Hz), 132.37 (CH, t, J_{CP} 4.5 Hz), 132.86 (CH, m), 133.09 (CH, m), 134.78 (C), 134.93 (C), 140.44 (C, t, J_{CP} 43.8 Hz), 141.19 (C, t, J_{CP} 43.2 Hz), 148.81 (C), 150.34 (C) ppm. ^{31}P NMR (CD$_2$Cl$_2$) δ: $+58.6$ (br s) ppm. FAB-MS: 751.4 (M–Cl, 100%); the isotopic pattern observed is as expected for $C_{44}H_{40}ClN_2NiP_2$.

3.4.3. (1,12-Dimethyl-5,8-diphenylbenzo[f]dinaphtho[2,1-m:1',2'-o]-1,12-diaza-5,8-diphosphacyclohexa-deca-6,13,15-triene)nickel(II)-dichloride (11A · NiCl$_2$)

45 mg (78%, orange crystals). ^{1}H NMR δ: 1.66 (m, 1H), 1.91 (m, 2H), 1.99 (s, 3H), 2.02 (m, 1H), 2.21 (m,

3H), 2.68 (s, 3H), 2.89 (m, 4H), 3.71 (m, 1H), 6.96 (t, 2H, J 9.3 Hz), 7.10 (d, 1H, J 8.5 Hz), 7.18 (m, 2H), 7.34 (m, 3H), 7.43 (m, 5H), 7.51 (m, 3H), 7.64 (m, 4H), 7.72 (m, 2H), 7.75 (br d, 1H, J 8.5 Hz), 7.85 (d, 1H, J 8.9 Hz), 7.94 (d, 1H, J 8.1 Hz), 8.13 (d, 1H, J 8.9 Hz) ppm. ^{13}C NMR δ: 22.93 (CH$_2$), 23.23 (CH$_2$), 23.39 (CH$_2$, d, J_{CP} 24.8 Hz), 23.71 (CH$_2$, d, J_{CP} 23.5 Hz), 41.07 (CH$_3$), 41.59 (CH$_3$), 55.21 (CH$_2$, d, J_{CP} 14.2 Hz), 56.80 (CH$_2$, d, J_{CP} 11.9 Hz), 119.83 (CH), 121.62 (CH), 123.66 (CH), 123.85 (CH), 125.79 (CH), 125.92 (CH), 126.10 (CH), 126.31 (CH), 126.91 (C), 127.41 (CH), 127.87 (CH), 128.25 (CH), 128.33 (C), 128.81 (2CH, d, J_{CP} 10.6 Hz), 129.47 (C, d, J_{CP} 52.6 Hz), 129.56 (C), 129.82 (CH), 130.29 (C), 130.33 (C, part of a d), 131.25 (CH), 131.28 (CH), 131.53 (CH, d, J_{CP} 14.9 Hz), 131.92 (CH, d, J_{CP} 15.0 Hz), 132.18 (CH, d, J_{CP} 9.2 Hz), 132.34 (CH, d, J_{CP} 8.9 Hz), 132.51 (CH, d, J_{CP} 5.2 Hz), 133.03 (CH, d, J_{CP} 5.1 Hz), 134.58 (C), 134.80 (C), 141.28 (C, dd, J_{CP} 36.6, 47.5 Hz), 142.92 (C, dd, J_{CP} 36.7, 48.6 Hz), 147.81 (C), 149.54 (C) ppm. ^{31}P NMR δ: $+60.1$, $+61.5$ (AB-system, J_{AB} 71.7 Hz) ppm. FAB-MS: 817.5 (M$^+$H, 100%); the isotopic pattern observed is as expected for $C_{46}H_{45}Cl_2N_2NiP_2$. Anal. Found: C, 66.61; H, 5.20; N, 3.35%. $C_{46}H_{44}Cl_2N_2NiP_2$ Calc.: C, 67.67; H, 5.43; N, 3.43%.

3.5. Asymmetric catalytic reactions (standard procedures)

3.5.1. Reaction (1), Procedure I [8a]

A dried 80 ml Schlenk tube was charged with 10 ml of dry Et$_2$O. After adding NiCl$_2$ (4.6 mg, 0.04 mmol, 0.5 mol%) and the ligand (0.04 mmol, 0.5 mol%) the mixture was degassed. A small Schlenk tube with calibration was cooled to 0 °C and vinyl bromide (0.5 ml, 7.1 mmol) was allowed to condense. The catalyst solution was cooled to -78 °C and vinyl bromide and 1-phenylethyl magnesium chloride (11.8 mmol, 1.7 equiv., solution 0.42 molar in Et$_2$O) was added subsequently while stirring. The Schlenk tube was carefully sealed and immersed into an ice bath. After 20 h the reaction was quenched by dropwise addition of 2 N HCl. The organic layer was separated and the aqueous layer was extracted with Et$_2$O (3 × 20 ml). The combined extracts were washed (saturated NaHCO$_3$, water, brine) and dried (Na$_2$SO$_4$). The solvent was removed under vacuo at RT and the residue was Kugelrohr distilled (bath temperature T_{max} 120 °C, 20 Torr). ^{1}H NMR showed the presence of minor amounts of ethyl benzene and styrene. The chemical yield was corrected accordingly. ^{1}H NMR δ: 1.36 (d, 3H, J 6.9 Hz), 3.47 (m, 1H), 5.04 (m, 2H), 6.01 (ddd, 1H, J 6.4, 10.3, 16.7 Hz), 7.19 (m, 3H), 7.30 (m, 2H) ppm. The enantiomeric excess was estimated using enantioselective GC [21] (Lipodex C*, FS, 0.25 mm × 50 m, 1 atm H$_2$, column

28–30 °C, injector 175 °C, split 1 : 100, sample 30 mg in 1 ml of CH_2Cl_2, 0.5 μl injected).

3.5.2. Reaction (2), Procedure II [9a]

To a degassed solution of allyl phenyl ether (2.68 g, 2.74 ml, 20 mmol) in 20 ml of dry Et_2O was added $NiCl_2$ (5 mg, 0.04 mmol, 0.2 mol%) and the ligand (0.04 mmol, 0.2 mol%). After stirring for 20 min the mixture was cooled in an ice bath and a solution of 1-phenylethyl magnesium chloride (20 mmol of a 0.42 molar solution in Et_2O) was added dropwise. The ice bath was removed and the mixture was stirred at RT. The progress of the conversion was followed by NMR. The reaction was quenched by careful addition of dilute HCl. The organic layer was separated and the aqueous layer was extracted repeatedly with Et_2O. The organic extracts were shaken with NaOH solution (10%) to remove phenol, washed neutral and dried (Na_2SO_4). The solvent was evaporated under vacuo at RT and the residue was subjected to Kugelrohr distillation to remove the catalyst and 2,3-diphenylbutane (bath temperature T_{max} 125 °C at 25 Torr). The distillate was filtered over a short column to remove traces of allyl phenyl ether and/or polar impurities (silica gel, 15 × 2.2 cm^2, PE). ^1H NMR δ: 1.25 (d, 3H, J 6.9 Hz), 2.21–2.32 (m, 1H), 2.34–2.42 (m, 1H), 2.74–2.83 (m, 1H), 4.94–5.01 (m, 2H), 5.66–5.76 (m, 1H), 7.18 (m, 3H), 7.29 (m, 2H) ppm. The enantiomeric excess was estimated using enantioselective GC [22] (50% Octakis(6-O-methyl-2,3-di-O-pentyl)-γ-cyclodextrin, FS, 0.25 mm × 25 m, 0.5 atm H_2, column 60 °C, injector 175 °C, split 1 : 100, sample 30 mg in 1 ml of CH_2Cl_2, 0.5 μl injected).

3.5.3. Reaction (3), Procedure IIIA (with BSA)

A solution of $[Pd(\eta^3\text{-}C_3H_5)Cl]_2$ (1.8 mg, 0.005 mmol, 1 mol% Pd) and the appropriate ligand (0.01 mmol, 1 mol%) was prepared in 1 ml of degassed CH_2Cl_2. To this pale yellow solution were subsequently added under argon 1 mmol of substrate (252 mg of (E)-1,3-diphenylprop-3-ene-1-yl acetate, 128 mg of (E)-pent-3-ene-2-yl acetate respectively), dimethyl malonate (396 mg, 340 μl, 3 mmol), BSA (610 mg, 741 μl, 3 mmol) and a catalytic amount of KOAc. The reaction mixture was degassed and then stirred at RT. In the case of (E)-1,3-diphenylprop-3-ene-1-yl acetate as substrate, the progress of the reaction was monitored via TLC (R_f 0.32 (educt), 0.11 (product), PE/EE 95 : 5). The reaction was stopped by adding 15 ml of Et_2O and the organic layer was washed twice with saturated NH_4Cl solution and dried (Na_2SO_4). The solvent was removed and the remaining yellow oil was chromatographed on silica gel.

14. Column chromatography (silica gel, 25 × 2.5 cm^2, PE/Et_2O 75 : 25, UV 220 nm). The isolated product was found to be pure by NMR. ^1H NMR δ: 1.00 (d, 3H, J 5.9 Hz), 1.59 (d, 3H, J 5.4 Hz), 2.86 (m, 1H),

3.24 (d, 1H, J 8.8 Hz), 3.66 (s, 3H), 3.70 (s, 3H), 5.30 (m, 1H), 5.49 (dq, 1H, J 6.4, 9.3 Hz) ppm. The enantiomeric excess was estimated by using enantioselective GC (50% Octakis(6-O-methyl-2,3-di-O-pentyl)-γ-cyclodextrin, FS, 0.25 mm × 25 m, 0.5 atm H_2, column 55 °C, injector 175 °C, split 1 : 100, sample 30 mg in 1 ml of CH_2Cl_2, 0.5 μl injected. Specific rotation calculated for optically pure **14**: $[\alpha]_D^{23}$ ±27.9 {c = 1.1, $CHCl_3$} [5i].

15. Column chromatography (silica gel, 10 × 2.2 cm^2, PE/CH_2Cl_2 50 : 50, UV 290 nm). The isolated product was found to be pure by NMR. ^1H NMR δ: 3.50 (s, 3H), 3.69 (s, 3H), 3.94 (d, 1H, J 10.8 Hz), 4.25 (dd, 1H, J 8.4, 10.8 Hz), 6.31 (dd, 1H, J 8.4, 15.8 Hz), 6.46 (d, 1H, J 15.8 Hz), 7.16–7.35 (m, 10H) ppm. E.e. was estimated by using a chiral shift reagent ($Eu(hfc)_3$, ^1H NMR in $CDCl_3$, integration of one singlet of diastereotopic OCH_3 groups which shifted from 3.67 to ca. 4.0 ppm, Δ 0.06–0.08 ppm) and was confirmed by chiral HPLC (Chiralcel OD-H, 250 × 4.6 mm^2, 0.5 ml min^{-1}, 2-propanol/n-hexane (2 : 98)). Specific rotation calculated for optically pure (S)-**15**: $[\alpha]_D^{20}$ −22.4 {c = 1.8, $CHCl_3$} [5h].

3.5.4. Reaction (3), Procedure IIIB with NaH

A solution of (E)-1,3-diphenylprop-3-ene-1-yl acetate (252 mg, 1 mmol) in 4 ml of dry THF was degassed, the isolated palladium complex L^*PdCl_2 ($L^* = $ **2A–6A**, 0.01 mmol, 1 mol%) [6] was added and the solution was stirred for 15 min [23]. A solution of the malonate anion was prepared at RT by adding NaH dispersion (63 mg, 1.5 mmol) in portions to a degassed solution of dimethyl malonate (198 mg, 171 μl, 1.5 mmol) in 4 ml of THF. After 30 min the resulting turbid solution was added to the ice cooled solution containing allyl acetate and the catalyst and the reaction was stirred at RT. The reaction was quenched by adding a small amount of 2 N HCl and the mixture was extracted with Et_2O (3 × 10 ml). The combined extracts were washed with brine until neutral and dried (Na_2SO_4). After removal of the solvent the crude product was purified by chromatography as given for Procedure IIIA.

3.6. X-ray structural analyses

Data were collected on a modified STOE diffractometer equipped with an N_2-cold-stream low temperature device (92 K) using Mo Kα radiation. Structure solutions were carried out by direct methods (SHELXTL-PC [24a]) followed by least-squares refinement against F^2 with no σ-cutoff being applied (SHELXL-93 [24b]). Anisotropic atomic displacement parameters (adps) were assigned to all non-hydrogen atoms. Positions of hydrogen atoms were calculated according to stereochemical aspects. Atomic coordinates are listed in Tables 4–6 [25].

Table 4

Atomic coordinates ($\times 10^4$) and equivalent isotropic displacement parameters ($\mathring{A}^2 \times 10^3$) for 2A

Atom	x	y	z	$U_{(eq)}$
P(1)	1118(2)	2415(1)	299(2)	22(1)
O(2)	2148(6)	3048(3)	3274(5)	23(1)
C(3)	2209(9)	2404(4)	3251(9)	23(2)
C(4)	2548(9)	2215(4)	1879(9)	24(2)
C(11)	1452(9)	3921(4)	4221(8)	19(2)
C(12)	1555(9)	3306(4)	4268(8)	19(2)
C(13)	1066(9)	2974(4)	5281(8)	22(2)
C(14)	397(9)	3266(4)	6187(9)	23(2)
C(15)	241(9)	3877(4)	6161(9)	23(2)
C(16)	−477(8)	4186(5)	7075(9)	24(2)
C(17)	−630(9)	4785(5)	7025(9)	28(2)
C(18)	−72(9)	5130(5)	6091(8)	27(2)
C(19)	624(9)	4851(4)	5186(9)	22(2)
C(20)	762(8)	4225(4)	5163(9)	22(2)
C(21)	1627(9)	1922(4)	−986(9)	25(2)
C(22)	915(10)	1406(4)	−1518(9)	27(2)
C(23)	2833(9)	2096(4)	−1479(9)	25(2)
C(24)	1373(10)	1068(5)	−2538(10)	33(2)
C(25)	3307(10)	1759(4)	−2447(9)	27(2)
C(26)	2596(10)	1246(5)	−2981(9)	30(2)
C(31)	−519(9)	2040(4)	631(8)	21(2)
C(32)	−423(9)	1468(4)	1198(9)	23(2)
C(33)	−1702(9)	1171(4)	1319(9)	25(2)
P(51)	−1986(2)	3093(1)	−448(2)	22(1)
O(52)	−462(5)	4533(3)	2026(6)	23(1)
C(53)	−1277(9)	4187(4)	860(9)	24(2)
C(54)	−1058(9)	3531(4)	1106(9)	22(2)
C(61)	1996(9)	4279(4)	3175(8)	19(2)
C(62)	1038(9)	4579(4)	2123(9)	21(2)
C(63)	1516(9)	4963(4)	1216(9)	26(2)
C(64)	2957(9)	5051(4)	1328(9)	22(2)
C(65)	4011(9)	4755(4)	2373(9)	21(2)
C(66)	5528(10)	4830(5)	2495(9)	29(2)
C(67)	6535(10)	4520(5)	3502(9)	28(2)
C(68)	6062(9)	4126(5)	4415(9)	28(2)
C(69)	4595(9)	4060(4)	4344(9)	23(2)
C(70)	3544(9)	4358(4)	3308(8)	19(2)
C(71)	3883(9)	3293(4)	−540(9)	23(2)
C(72)	4484(9)	3341(4)	632(9)	25(2)
C(73)	4748(9)	3460(4)	−1835(9)	25(2)
C(74)	5893(10)	3535(4)	485(9)	26(2)
C(75)	6173(9)	3658(5)	−1987(9)	28(2)
C(76)	6727(9)	3710(5)	−809(9)	28(2)
C(81)	1842(8)	2341(5)	237(8)	24(2)
C(82)	3099(9)	2013(4)	341(9)	25(2)
C(83)	3016(9)	1433(4)	843(9)	25(2)
O(91)	2935(7)	166(3)	2270(7)	39(2)
C(92)	3389(11)	514(5)	1100(11)	41(2)
C(93)	4021(11)	645(6)	3552(11)	50(3)
C(94)	4508(12)	65(6)	1700(12)	53(3)
C(95)	5314(11)	367(6)	3117(12)	59(4)
O(101)	5804(8)	1996(5)	5654(9)	66(2)
C(102)	7068(14)	1650(7)	6166(13)	64(3)
C(103)	6291(13)	2487(7)	5057(14)	63(3)
C(104)	8017(13)	1741(6)	5155(12)	55(3)
C(105)	7304(13)	225(6)	4220(12)	56(3)

$U_{(eq)}$ is defined as one third of the trace of the orthogonalized U_{ij} tensor.

2A. Slow evaporation of a concentrated THF solution of (S)-2A afforded flat plates which easily lose solvent upon exposure to air. The crystals are monoclinic, space

group $P2(1)$; $a = 9.436(2)$, $b = 22.421(4)$, $c = 9.828(4)$, $\beta = 104.33(3)$, $V = 2014.6(7)$ $\mathring{A}^3$, $Z = 2$, $d_{calc} = 1.281$ g cm^{-3}, maximum 2θ for data collection 45°. Refinement of 504 parameters against 2758 intensity

Table 5

Atomic coordinates ($\times 10^4$) and equivalent isotropic displacement parameters ($\mathring{A}^2 \times 10^3$) for 2A·PdCl$_2$

Atom	x	y	z	$U_{(eq)}$
Pd	5934(1)	7599(1)	7856(1)	14(1)
Cl(A)	6663(1)	6174(1)	8142(1)	24(1)
Cl(B)	5014(1)	7799(1)	8888(1)	21(1)
P(1)	6884(1)	7532(1)	6912(1)	16(1)
O(2)	8685(2)	8715(2)	7655(2)	18(1)
C(3)	8794(3)	7746(3)	7655(2)	21(1)
C(4)	8296(3)	7342(3)	7031(2)	20(1)
C(11)	8999(3)	10106(3)	8212(2)	16(1)
C(12)	9147(3)	9178(3)	8191(2)	16(1)
C(13)	9742(3)	8720(3)	8697(2)	20(1)
C(14)	10207(3)	9205(3)	9210(2)	20(1)
C(15)	10088(3)	10158(3)	9257(2)	18(1)
C(16)	10572(3)	10663(3)	9782(2)	21(1)
C(17)	10442(4)	11588(3)	9815(2)	22(1)
C(18)	9801(3)	12033(3)	9335(2)	21(1)
C(19)	9328(3)	11569(3)	8816(2)	18(1)
C(20)	9469(3)	10604(3)	8756(2)	14(1)
C(21)	6447(4)	6685(3)	6307(2)	21(1)
C(22)	7085(4)	5985(3)	6064(3)	32(1)
C(23)	5411(4)	6776(3)	6071(2)	26(1)
C(24)	6687(5)	5382(4)	5574(3)	40(1)
C(25)	5017(5)	6179(3)	5576(2)	32(1)
C(26)	5667(5)	5493(4)	5332(3)	39(1)
C(31)	6735(3)	8585(3)	6446(2)	17(1)
C(32)	7278(4)	8767(3)	5839(2)	23(1)
C(33)	7097(4)	9578(3)	5498(2)	24(1)
P(51)	5287(1)	8901(1)	7464(1)	14(1)
O(52)	6926(2)	10758(2)	8433(2)	21(1)
C(53)	6465(3)	9852(3)	8429(2)	21(1)
C(54)	5402(3)	9842(3)	8052(2)	19(1)
C(61)	8411(3)	10618(3)	7684(2)	16(1)
C(62)	7415(3)	10962(3)	7817(2)	19(1)
C(63)	6894(4)	11549(3)	7372(2)	23(1)
C(64)	7363(4)	11776(3)	6771(2)	25(1)
C(65)	8363(4)	11429(3)	6595(2)	21(1)
C(66)	8862(4)	11649(3)	5967(2)	24(1)
C(67)	9852(4)	11330(3)	5815(2)	26(1)
C(68)	10398(4)	10785(3)	6286(2)	24(1)
C(69)	9945(3)	10558(3)	6893(2)	19(1)
C(70)	8905(3)	10857(2)	7060(2)	17(1)
C(71)	3899(3)	8864(3)	7233(2)	16(1)
C(72)	3120(3)	8912(3)	7734(2)	20(1)
C(73)	3599(3)	8753(3)	6561(2)	20(1)
C(74)	2066(3)	8859(3)	7559(3)	23(1)
C(75)	2535(3)	8694(3)	6384(2)	24(1)
C(76)	1775(3)	8744(3)	6884(3)	23(1)
C(81)	5999(3)	9207(2)	6696(2)	15(1)
C(82)	5812(3)	10027(3)	6342(2)	19(1)
C(83)	6371(4)	10196(3)	5749(2)	22(1)
C(96)	7753(5)	7374(5)	9640(3)	16(1)
C(97)	7231(11)	6331(11)	9649(7)	29(3)
C(98)	7180(5)	6643(5)	9752(3)	38(1)

$U_{(eq)}$ is defined as one third of the trace of the orthogonalized U_{ij} tensor.

Table 6

Atomic coordinates (×10⁴) and equivalent isotropic displacement parameters ($\text{Å}^2 \times 10^3$) for 11A·NiCl₂

Atom	x	y	z	$U_{(eq)}$
Ni	753(1)	399(1)	2472(1)	18(1)
Cl(A)	297(2)	1768(2)	3227(2)	23(1)
Cl(B)	−895(2)	88(2)	1449(2)	28(1)
P(1)	2442(2)	670(2)	3399(2)	19(1)
N(2)	5993(7)	2089(5)	2372(5)	19(2)
C(3)	5828(9)	2653(7)	3281(6)	24(2)
C(4)	4878(9)	2086(7)	3792(6)	26(2)
C(5)	3560(9)	1707(7)	3228(6)	24(2)
C(11)	5987(8)	3143(6)	1343(6)	18(2)
C(12)	6643(8)	2626(6)	1774(6)	17(2)
C(13)	7978(8)	2604(7)	1631(6)	22(2)
C(14)	8621(8)	3066(7)	1038(6)	22(2)
C(15)	7971(8)	3551(6)	533(6)	14(2)
C(16)	8591(9)	3961(6)	−120(6)	18(2)
C(17)	7915(9)	4385(7)	−637(6)	23(2)
C(18)	6595(8)	4410(6)	−522(6)	21(2)
C(19)	5975(9)	4032(6)	139(6)	21(2)
C(20)	6633(8)	3585(6)	688(6)	17(2)
C(21)	2162(8)	817(7)	4585(6)	19(2)
C(22)	2131(9)	1718(8)	5143(6)	29(3)
C(23)	1858(9)	18(8)	4925(6)	29(3)
C(24)	1809(9)	1797(8)	6051(7)	33(3)
C(25)	1562(9)	118(8)	5824(7)	31(3)
C(26)	1522(9)	1001(9)	6391(7)	36(3)
C(31)	3287(8)	−329(6)	3112(6)	19(2)
C(32)	4394(9)	−406(7)	3634(7)	27(2)
C(33)	5032(9)	−1155(7)	3319(7)	27(2)
C(41)	6488(9)	1215(7)	2384(7)	29(3)
P(51)	1366(2)	−865(2)	1736(2)	19(1)
N(52)	3596(7)	1669(5)	742(5)	19(2)
C(53)	2522(9)	897(6)	738(7)	23(2)
C(54)	2951(8)	−49(6)	534(6)	21(2)
C(55)	1824(9)	−876(7)	584(6)	22(2)
C(61)	4633(8)	3298(7)	1567(6)	20(2)
C(62)	3515(9)	2581(6)	1273(6)	18(2)
C(63)	2282(8)	2782(7)	1561(6)	18(2)
C(64)	2165(8)	3641(7)	2081(6)	19(2)
C(65)	3252(9)	4390(6)	2351(6)	18(2)
C(66)	3148(10)	5299(7)	2878(6)	26(2)
C(67)	4197(10)	6014(7)	3135(7)	31(3)
C(68)	5443(10)	5839(7)	2909(7)	35(3)
C(69)	5595(9)	4958(7)	2398(6)	25(2)
C(70)	4499(8)	4206(6)	2092(6)	18(2)
C(71)	223(8)	−1975(6)	1602(6)	21(2)
C(72)	−803(9)	−2262(7)	919(6)	25(2)
C(73)	320(9)	−2567(7)	2190(6)	26(2)
C(74)	−1689(9)	−3103(7)	825(7)	26(2)
C(75)	−563(10)	−3418(7)	2084(7)	30(3)
C(76)	−1578(9)	−3684(7)	1397(7)	31(3)
C(81)	2836(8)	−1010(7)	2319(6)	19(2)
C(82)	3510(9)	−1756(7)	2004(7)	26(2)
C(83)	4605(9)	−1817(7)	2505(7)	29(3)
C(91)	4201(9)	1603(7)	−127(6)	27(2)
C(101)	522(17)	5914(18)	4197(15)	129(8)
C(102)	1479(26)	7203(16)	4650(8)	161(12)
C(104)	−2042(60)	5375(45)	4355(71)	102(126)
C(105)	3101(66)	4924(22)	5099(15)	570(61)

$U_{(eq)}$ is defined as one third of the trace of the orthogonalized U_{ij} tensor.

data converged at the following values for reliability indices: $wR_2 = \sum[w(F_o^2 - F_c^2)^2 / \sum[w(F_o^2)^2]] = 0.182$ for 2192 reflections, $R_1 = \sum ||F_o| - |F_c|| / \sum |F_o| = 0.067$ for 2758 reflections with $F_o > 4\sigma(F_o)$. There are two additional well-ordered THF molecules in the asymmetric unit.

2A·PdCl₂. From a dilute solution of (S)-2A and Pd(C₆H₅CN)₂Cl₂ in CH₂Cl₂/EtOH grew colorless prisms after several days. The crystals are orthorhombic, space group $P2(1)2(1)2(1)$; $a = 12.572(3)$, $b = 14.640(5)$, $c = 19.617(4)$, $V = 3610.6(14)$ Å³, $Z = 4$, $d_{calc} = 1.490$ g cm⁻³, maximum 2θ for data collection 60°. Refinement of 490 parameters against 6397 intensity data converged at the following values for reliability indices: $wR_2 = \sum[w(F_o^2 - F_c^2)^2 / \sum[w(F_o^2)^2]] = 0.106$ for 6397 reflections, $R_1 = \sum ||F_o| - |F_c|| / \sum |F_o| = 0.038$ for 5925 reflections with $F_o > 4\sigma(F_o)$.

11A·NiCl₂. From a solution of racemic 11A and NiCl₂·6H₂O in CH₂Cl₂/EtOH grew needle-like orange–brown crystals after a few hours. The crystals are triclinic, space group $P\bar{1}$; $a = 10.379(2)$, $b = 14.695(2)$, $c = 15.146(3)$, $\alpha = 103.98(3)$, $\beta = 91.53(3)$, $\gamma = 100.23(3)$, $V = 2220.1(8)$ Å³, $Z = 2$, $d_{calc} = 1.305$ g cm⁻³, maximum 2θ for data collection 46°. Refinement of 515 parameters against 4565 intensity data converged at the following values for reliability indices: $wR_2 = \sum[w(F_o^2 - F_c^2)^2 / \sum[w(F_o^2)^2]] = 0.211$ for 4565 reflections, $R_1 = \sum ||F_o| - |F_c|| / \sum |F_o| = 0.068$ for 3141 reflections with $F_o > 4\sigma(F_o)$.

The structures of 2A·PdCl₂ and 11A·NiCl₂ contain disordered solvent and several dummy atoms were introduced to account for residual electron density.

4. Conclusions

The general usefulness of macrocyclic diphosphine ligands has been demonstrated for the palladium catalyzed allylic substitution provided one of the allylic intermediates, stabilized by steric and/or electronic interactions, predominates. Their absence for substrates like (E)-pent-3-ene-2-yl acetate or cyclohex-1-ene-3-yl acetate seems to be responsible for poor e.e. values. An improvement can be expected for more rigid ligand structures with enlarged perimeter, eventually forcing the allyl complex into better proximity to the chiral environment. Assuming Curtin–Hammett conditions and the enantioselective step to be under reactant control, the sense and magnitude of the asymmetric induction will be the result of both the preference of one allylic intermediate and the regioselectivity of the nucleophilic attack.

Acknowledgements

References and notes

[1] I. Ojima (ed.), *Catalytic Asymmetric Synthesis*, VCH, Weinheim, 1993.

[2] H. Brunner and W. Zettlmeier, *Handbook of Enantioselective Catalysis*, VCH, Weinheim, 1993.

[3] (a) T. Hayashi, M. Fukushima, M. Konishi and M. Kumada, *Tetrahedron Lett.*, *21* (1980) 79; (b) T. Hayashi, A. Yamamoto, M. Hojo and Y. Ito, *J. Chem. Soc., Chem. Commun.*, (1989) 495.

[4] T. Hayashi, K. Hayashizaki, T. Kiyoi and Y. Ito, *J. Am. Chem. Soc.*, *110* (1988) 8153.

[5] Cf. P–P ligands: (a) M. Yamaguchi, T. Shima, T. Yamagishi and M. Hida, *Tetrahedron: Asymm.*, *2* (1991) 663; (b) A. Togni, C. Breutel, A. Schnyder, F. Spindler, H. Landert and A. Tijani, *J. Am. Chem. Soc.*, *116* (1994) 4062. N–N ligands: (c) U. Leutenegger, G. Umbricht, C. Fahrni, P. von Matt and A. Pfaltz, *Tetrahedron*, *48* (1992) 2143; (d) H. Kobota, M. Nakajima and K. Koga, *Tetrahedron Lett.*, *34* (1993) 8135; (e) D. Tanner, P.G. Andersson, A. Harden and P. Somfai, *Tetrahedron Lett.*, *35* (1994) 4631; (f) P. Gamez, B. Dunjic, F. Fache and M. Lemaire, *Tetrahedron: Asymm.*, *6* (1995) 1109. P–N ligands: (g) G.J. Dawson, C.G. Frost, J.M.J. Williams and S.J. Coote, *Tetrahedron Lett.*, *34* (1993) 3149; (h) J. Sprinz and G. Helmchen, *Tetrahedron Lett.*, *34* (1993) 1769; (i) P. von Matt and A. Pfaltz, *Angew. Chem.*, *105* (1993) 614; (j) B.M. Trost and R.C. Bunt, *J. Am. Chem. Soc.*, *116* (1994) 4089; (k) J. Sprinz, M. Kiefer, G. Helmchen, M. Reggelin, G. Huttner, O. Walter and L. Zsolnai, *Tetrahedron Lett.*, *35* (1994) 1523; (l) G. Dawson, J.M.J. Williams and S.J. Coote, *Tetrahedron Lett.*, *36* (1995) 461; (m) H. Kubota and K. Koga, *Tetrahedron Lett.*, *35* (1994) 6689; (n) P. Wimmer and M. Widhalm, *Tetrahedron: Asymm.*, *6* (1995) 657.

[6] (a) M. Widhalm, H. Kalchhauser and H. Kühlig, *Helv. Chim. Acta*, *77* (1994) 409; (b) M. Widhalm and G. Klintschar, *Chem. Ber.*, *127* (1994) 1411; (c) cf. R.B. Kress, E.N. Duesler, M.C. Etter, I.C. Paul and D.Y. Curtin, *J. Am. Chem. Soc.*, *102* (1980) 7709.

[7] P. Wimmer and M. Widhalm, *Phosphorus, Sulfur and Silicon*, *106* (1995) 105.

[8] (a) T. Hayashi, M. Konishi, M. Fukushima, T. Mise, M. Kagotani, M. Tajika and M. Kumada, *J. Am. Chem. Soc.*, *104* (1982) 180; (b) J.M. Brown and N.A. Cooley, *Chem. Rev.*, *88* (1988) 1031; (c) J.M. Brown and N.A. Cooley, *Organometallics*, *9* (1990) 353; (d) A. Indolese and G. Consiglio, *J. Organomet. Chem.*, *463* (1993) 23.

[9] (a) G. Consiglio, O. Piccolo, L. Roncetti and F. Morandini, *Tetrahedron*, *42* (1986) 2043; (b) G. Consiglio and A. Indolese, *Organometallics*, *10* (1991) 3425.

[10] (a) B.M. Trost, *Acc. Chem. Res.*, *13* (1980) 385; (b) P.R. Auburn, P.B. Mackenzie and B. Bosnich, *J. Am. Chem. Soc.*, *107* (1985) 2033; (c) P.B. Mackenzie, J. Wehlan and B. Bosnich, *J. Am. Chem. Soc.*, *107* (1985) 2046; (d) [5k]; (e) J.M. Brown, D.I. Hulmes and P.J. Guiry, *Tetrahedron*, *50* (1994) 4493.

[11] J.V. Allen, J.F. Bower and J.M.J. Williams, *Tetrahedron: Asymm.*, *5* (1994) 1895.

[12] (a) M.F. Rettig and P.M. Maitlis, *Inorg. Synth.*, *2* (1943) 167; (b) K. Moseley and P.M. Maitlis, *J. Chem. Soc., Dalton Trans.*, (1974) 169.

[13] Highest asymmetric inductions reported: (E)-pent-3-ene-2-yl acetate, 97% e.e. [5i]; 3-acetoxy-cyclohexene, 96% e.e. [5j].

[14] (a) K. Tamao, Y. Kiso, K. Sumitani and M. Kumada, *J. Am. Chem. Soc.*, *94* (1972) 9268; (b) Y. Kiso, K. Tamao and M. Kumada, *J. Organomet. Chem.*, *50* (1973) C12.

[15] Molecular modelling experiments were performed on a Silicon Graphics Workstation using the program SYBYL (Trypos) version 6.2; details will be published elsewhere.

[16] L.I. Smith, H.H. Hoehn and A.G. Whitney, *J. Am. Chem. Soc.*, *62* (1940) 1863.

[17] F.G. Mann and A.J.H. Mercer, *J. Chem. Soc., Perkin Trans. I*, (1972) 1631.

[18] P. von Matt, O. Loiseleur, G. Koch, A. Pfaltz, C. Lefeber, T. Feucht and G. Helmchen, *Tetrahedron: Asymm.*, *5* (1994) 573.

[19] (a) M.H. Nomura, *Bull. Soc. Chem. Fr.*, *37* (1925) 1245; (b) [10b].

[20] H.-J. Lautenschlager, *Thesis*, Regensburg, 1989.

[21] H. Brunner, H.-J. Lautenschlager, W.A. König and R. Krebber, *Chem. Ber.*, *123* (1990) 847.

[22] W.A. König, in *Gas Chromatographic Enantiomer Separation with Modified Cyclodextrins*, Hüthig, Heidelberg, 1992.

[23] Palladium complexes of 10A and 11A were prepared in situ from ligands and Pd(OAc)₂.

[24] (a) G.M. Sheldrick, SHELXTL-PC, Release 4.1, Siemens Crystallographic Research Systems, 1990; (b) G.M. Sheldrick, SHELXL-93, a program for the refinement of crystal structures from diffraction data, University of Göttingen, 1993.

[25] Supplementary data (bond length, bond angles, torsional angles and structure factors) have been deposited at the Cambridge Crystallographic Data Centre.